Ultramicroscopy ■ (■■■■) ■■■–■■■

Contents lists available at ScienceDirect

Ultramicroscopy

journal homepage: www.elsevier.com/locate/ultramic

Imaging of radiation damage using complementary field ion microscopy and atom probe tomography

Michal Dagan [a,*], Luke R. Hanna [a], Alan Xu [a], Steve G. Roberts [a,b], George D.W. Smith [a], Baptiste Gault [a], Philip D. Edmondson [a,1], Paul A.J. Bagot [a], Michael P. Moody [a]

[a] Department of Materials, University of Oxford, Parks Road, Oxford OX1 3PH, UK
[b] Culham Centre for Fusion Energy, Culham Science Centre, Abingdon OX14 3DB, UK

ARTICLE INFO

Article history:
Received 30 August 2014
Received in revised form
22 January 2015
Accepted 26 February 2015

Keywords:
Field ion microscopy
Atom probe tomography
Radiation damage
Crystal defects
Tungsten
Tungsten–tantalum alloy

ABSTRACT

Radiation damage in tungsten and a tungsten–tantalum alloy, both of relevance to nuclear fusion research, has been characterized using a combination of field ion microscopy (FIM) imaging and atom probe tomography (APT). While APT provides 3D analytical imaging with sub-nanometer resolution, FIM is capable of imaging the arrangements of single atoms on a crystal lattice and has the potential to provide insights into radiation induced crystal damage, all the way down to its smallest manifestation – a single vacancy. This paper demonstrates the strength of combining these characterization techniques. In ion implanted tungsten, it was found that atomic scale lattice damage is best imaged using FIM. In certain cases, APT reveals an identifiable imprint in the data via the segregation of solute and impurities and trajectory aberrations. In a W–5 at%Ta alloy, a combined APT–FIM study was able to determine the atomic distribution of tantalum inside the tungsten matrix. An indirect method was implemented to identify tantalum atoms inside the tungsten matrix in FIM images. By tracing irregularities in the evaporation sequence of atoms imaged with FIM, this method enables the benefit of FIM's atomic resolution in chemical distinction between the two species.

1. Introduction

Nuclear fission power currently provides over 11% of the world's electricity demands and allows reliable electricity production, with negligible CO_2 emissions [1]. As nuclear fusion becomes increasingly recognized as a potential alternative to fission, great efforts are being made worldwide towards developing nuclear fusion reactors. These are aimed to offer a secure source of energy with no production of greenhouse gases, no long-lived radioactive waste and almost unlimited fuel supplies. In particular, ITER, a major international effort to build a commercial reactor-scale fusion device, is currently undergoing construction [2]. Both fission and fusion reactors operate in a highly aggressive environment of high temperatures and high doses of energetic neutrons [3–7]. Bombardment by neutrons, characteristic of these environments, initializes atomic scale changes in the microstructures of the materials inside the reactor. Primary mechanisms of such initial changes are either displacement of atoms from their lattice positions by neutron collisions [8], or the generation of hydrogen and helium through chemical transmutation reactions that cluster into bubbles leading to undesirable swelling of the matrix [7]. These initial atomic scale changes further develop into a variety of chemical and structural features [9,10] which can ultimately undermine critical mechanical properties through phenomena such as radiation induced embrittlement [11], radiation hardening [12] and radiation induced clustering [10]. It is therefore crucial to fully understand mechanisms that are in operation from even the earliest stages of atomic scale damage. Such knowledge will allow the accurate evaluation of operational lifetime of the different components, and the development of new, sustainable materials towards internal components of nuclear reactors.

Atom probe tomography (APT) has been established over the past decades as a key technique for the characterization of radiation-induced nanoscale damage in materials for fission and fusion applications [13]. Among these, case studies include radiation-induced clustering in reactor pressure vessels (RPV) steels [14–16], particle stability and distribution of oxide particles in oxide dispersion strengthened steels (ODS) [17–19], helium bubble trapping at oxide particles in ODS steels [20] and surface oxidation processes of stainless steels [21] and zirconium alloys [22] in corrosive environment. With the rise to prominence of APT, the potential of its forerunner, field ion microscopy (FIM), has largely been overlooked. While APT has proven capabilities for the study of small

* Corresponding author.
E-mail address: Michal.dagan@materials.ox.ac.uk (M. Dagan).
[1] Current address: Oak Ridge National Laboratory, One Bethel Valley Road, Oak Ridge, TN 378316140, USA.

http://dx.doi.org/10.1016/j.ultramic.2015.02.017
0304-3991/

scale radiation induced chemical changes, it lacks the necessary spatial resolution and detection efficiency to image individual sites on the crystal lattice and therefore struggles in the direct imaging of atomic scale crystal damage. FIM, on the other hand, is comparatively more limited in terms of analytical capabilities. However, it enables direct imaging of complete crystallographic arrangements of atoms on the surface of the sample and can therefore constitute as a highly beneficial complementary technique to APT.

FIM and APT are based upon the concept of field ionization and field evaporation respectively [23]. Both techniques require a very sharp needle-shaped specimen, held in an ultra-high vacuum chamber, and exploit the fact that an intense electric field can be generated at its apex by application of a DC voltage. In APT, high voltage/laser light pulses are superimposed on the standing DC voltage to trigger the field evaporation of atoms on the surface of the specimen, which are in turn projected onto a position-sensitive detector. Each hit on the detector can be directly related to the pulse responsible for the single corresponding field evaporation event, facilitating highly accurate time-of-flight measurements and hence chemical identification. In the final step an inverse projection algorithm, combined with the sequence of evaporation and an assumed model for specimen shape enable a 3D atom-by-atom reconstruction of the analyzed volume [24].

In the case of FIM, the analysis chamber also contains inert imaging gas atoms at a pressure of approximately 10^{-5} mbar. The gas atoms are polarized by the electric field and are drawn to the tip, forming an adsorbed layer of atoms on the surface. If the electric field is sufficiently high, gas atoms above the specimen are ionized and projected onto a phosphor screen, producing a highly magnified image of the surface of the specimen. A typical FIM image of a tungsten sample oriented along the [011] direction is presented in Fig. 1b. Each spot in the image represents the position of an individual atom on the surface of the tip. Since more gas ions originate from the vicinity of the most protruding atoms, these locations are preferentially imaged and a terrace pattern is formed. Ultimately, the FIM image represents an atomic resolution quasi-stereographic projection of the crystal. If the applied electric field is increased sufficiently, atoms from the specimen itself can be field evaporated from the surface. In this way the specimen can be probed in depth, atom-by-atom and layer-by-layer enabling characterization of the internal microstructure.

Ground-breaking FIM studies in the 1960s–1980s previously demonstrated the direct imaging of radiation-induced voids, dislocations, self-interstitials, and single vacancies in the crystal lattice and brought significant new insights to the full spatial characterization of radiation-induced depleted zones [25–30]. However, these studies all predated digital imaging. While in the meantime little has changed in terms of FIM instrumentation, the capacity to capture such images digitally presents an array of new possibilities in terms of data collection, and tailored data analysis.

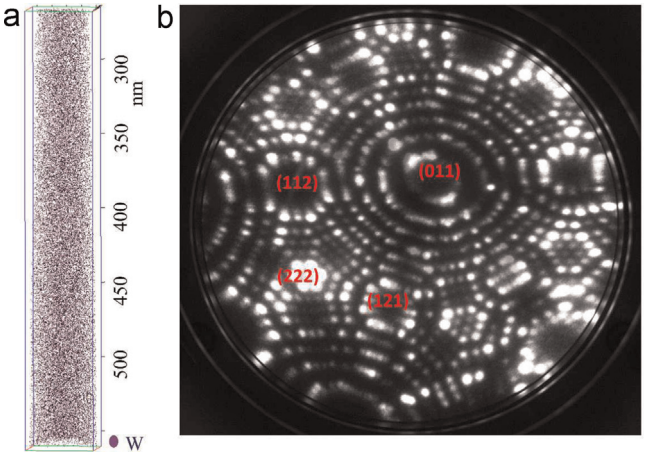

Fig. 1. APT and FIM results obtained for the reference un-implanted tungsten samples. (a) Homogenous tungsten matrix seen in the APT reconstruction. For clarity, 0.3% of the atoms are presented in a characteristic 300 nm long part of the reconstruction. (b) Characteristic bcc lattice imaged with FIM and helium as the imaging gas. Some of the main poles are indexed. Both measurements were taken at 50 K.

In this study, we explore potential applications and data analysis techniques for both FIM and APT. Firstly, we demonstrate combined APT/FIM study of radiation-induced crystal damage in tungsten samples. Tungsten is considered as a prime candidate material for different plasma facing components of future fusion reactors due to its high melting point, high thermal conductivity, low expansion coefficient and low erosion rate [31]. In particular, tungsten is being investigated for the use in the divertor and the first wall protection layer for future Tokamak based fusion reactors including and going beyond ITER [11,32,33].

Furthermore, an un-irradiated W–5 at%Ta alloy (hereafter termed 'W–5Ta') was also studied, and FIM analysis was developed to achieve atomic scale mapping of the distribution of solute tantalum atoms inside the tungsten matrix. The characterization of tungsten–tantalum alloys is of particular interest for fusion reactors as tantalum is a product of tungsten transmutation. Under ITER conditions, simulations show that about 0.6 at% tantalum will be formed from pure tungsten over the first five years of operation of commercial reactors [34]. Previous studies of W–5Ta have shown increased hardness post ion-implantation [35]. A similar phenomenon in W–5 at%Re alloys was found to be the result of radiation-induced solute clustering revealed by APT [36], which could indicate a potential reason for currently unexplained measured increase in W–5Ta hardness. The W–5Ta alloy was chosen here to demonstrate an atomic scale spatial distribution FIM technique that will potentially allow the detection of early stage clustering in FIM, beyond the APT detection power.

Contributions from both FIM and APT approaches used here for the study of tungsten, and tungsten–tantalum alloys are compared and discussed as well as future directions for complementary characterization protocols for APT/FIM.

2. Materials and Experiment

Tungsten samples (purity level >99.9 at%) were electropolished in a 5%NaOH solution from a tungsten wire oriented along the [011] direction, into sharp needle-shaped specimens, with an estimated apex radius of less than 50 nm. To simulate displacement damage from neutron bombardment [37,38], the electropolished-needle specimens were subject to various tungsten ion implantations to create displacement cascades in the crystal lattice at increasing levels of damage. Ion implantation is a commonly used proxy to model the effects of neutron irradiation within material systems and is usually a safer and more cost effective approach. Importantly, under controlled temperature and radiation rate conditions, in a matter of hours, ion irradiation can be used to induce radiation damage profiles that are characteristic of that induced by exposure to many years of reactor operation. While the nature of the interaction with the lattice, and as a result the scattering cross section and the penetration depth, are different in the ionic and neutral cases, there is ongoing work to investigate the validity of this widely used approximation and to optimize its application [39,40]. However, for the current study, seeking to characterize the broadly defined regimes of low, medium and high levels of damage, the profile damage that is produced from ion implantation remains a good approximation.

Further, W–5Ta alloy samples were also prepared from a W–

Please cite this article as: M. Dagan, et al., Imaging of radiation damage using complementary field ion microscopy and atom probe tomography, Ultramicroscopy (2015), http://dx.doi.org/10.1016/j.ultramic.2015.02.017